Dalton Transactions

PAPER

View Article Online
View Journal

Cite this: DOI: 10.1039/c6dt02239a

Organic derivatives of $Mg(BH_4)_2$ as precursors towards MgB_2 and novel inorganic mixed-cation borohydrides†‡

W. Wegner,[a,b] T. Jaroń,*[a] M. A. Dobrowolski,[c] Ł. Dobrzycki,[c] M. K. Cyrański[c] and W. Grochala*[a]

Received 4th June 2016,
Accepted 31st July 2016

DOI: 10.1039/c6dt02239a

www.rsc.org/dalton

A series of organic derivatives of magnesium borohydride, including $Mg(BH_4)_2$·1.5DME (DME = 1,2-dimethoxyethane) and $Mg(BH_4)_2$·3THF (THF = tetrahydrofuran) solvates and three mixed-cation borohydrides, $[Cat]_2[Mg(BH_4)_4]$, [Cat] = $[Me_4N]$, $[nBu_4N]$, $[Ph_4P]$, have been characterized. The phosphonium derivative has been tested as a precursor for synthesis of inorganic mixed-metal borohydrides of magnesium, $M_x[Mg(BH_4)_{2+x}]$, M = Li–Cs, *via* a metathetic method. The synthetic procedure has yielded two new derivatives of heavier alkali metals $M_3Mg(BH_4)_5$ (M = Rb, Cs) mixed with amorphous $Mg(BH_4)_2$. Thermal decomposition has been studied for both the organic and inorganic magnesium borohydride derivatives. Amorphous MgB_2 has been detected among the products of the thermal decomposition of the solvates studied, together with organic and inorganic impurities.

Introduction

Storage of hydrogen in chemical compounds is one of the methods being currently employed for the use of hydrogen as an energy carrier.[1–5] Consequently, diverse types of potential chemical hydrogen stores have been investigated with a significant intensification of efforts observed over the last two decades.[6] Hydrogen-rich borohydrides have attracted attention revealing a higher relative amount of hydrogen than the other groups of simple inorganic compounds containing the same cations.[7] Although none of the currently known borohydrides can be directly used as a hydrogen store (which is caused predominantly by either too easy or too difficult release of hydrogen, poor reversibility of storage and contamination of released hydrogen by B_2H_6),[8] the interest in H-rich borohydrides stimulated many recent developments.[9–12]

Magnesium borohydride, $Mg(BH_4)_2$, due to its high content of hydrogen (14.9 wt%), worldwide prevalence and the low price of magnesium, is an important prototype material for hydrogen storage.[13] Several routes of its synthesis have been elaborated yielding five known polymorphs of $Mg(BH_4)_2$.[9,14–18] Hydrogen evolution from pure $Mg(BH_4)_2$ requires heating above *ca.* 290 °C, while above *ca.* 450 °C MgB_2 can be detected as the final product of the multi-step dehydrogenation process.[19] Diverse methods have been tested to enhance the hydrogen release from $Mg(BH_4)_2$, which includes amorphization, dispersion in a porous matrix, and preparation of composites with various additives.[19] These studies led to the discovery of mixed-metal borohydrides containing magnesium, as represented by solid solutions, *e.g.* $Mg_xMn_{(1-x)}(BH_4)_2$, $RbMg_xCa_{(1-x)}(BH_4)_3$,[20,21] bimetallic borohydrides, such as $K_2Mg(BH_4)_4$, $K_3Mg(BH_4)_5$ and $CsMg(BH_4)_3$,[21,22] as well as more complex borohydrides, like $LiKMg(BH_4)_4$, $LiRbMg(BH_4)_4$, $Li_2K_3Mg_2(BH_4)_9$ and $Li_3MgZn_5(BH_4)_{15}$.[23,24]

Here we have extended the earlier characterization of several organic derivatives of magnesium borohydride: $[Cat]_2[Mg(BH_4)_4]$, [Cat] = $[Me_4N]$, $[nBu_4N]$, $[Ph_4P]$, as well as $Mg(BH_4)_2$·1.5DME and $Mg(BH_4)_2$·3THF solvates, where DME – 1,2-dimethoxyethane and THF – tetrahydrofuran.[25–27] The latter two show very good solubility in diverse organic solvents and their solutions exhibit a broad range of volatility and viscosity. Therefore, we have studied their thermal decomposition to verify whether they might be used as precursors towards superconducting layers of MgB_2 on neutral substrates.[28–30]

[a]*Centre of New Technologies, University of Warsaw, Żwirki i Wigury 93, 02089 Warsaw, Poland. E-mail: tjaron@uw.edu.pl, w.grochala@cent.uw.edu.pl*
[b]*College of Inter-Faculty Individual Studies in Mathematics and Natural Sciences, University of Warsaw, Stefana Banacha 2C, 02-097 Warsaw, Poland*
[c]*Advanced Crystal Engineering Laboratory (aceLAB), University of Warsaw, Faculty of Chemistry, Żwirki i Wigury 101, 02089 Warsaw, Poland*

†Electronic supplementary information (ESI) available: Synthetic procedures, PXRD patterns, FTIR & XPS & MS spectra. Details of the crystal structure of $Mg(BH_4)_2$·1.5DME may be obtained from the Cambridge Crystallographic Data Centre *via* http://www.ccdc.cam.ac.uk/data_request/cif on quoting the CCDC number 1482748. For ESI and crystallographic data in CIF or other electronic format see DOI: 10.1039/c6dt02239a

‡Details of the crystal structure of $M_3[Mg(BH_4)_5]$, M = Rb, Cs, may be obtained from Fachinformationszentrum Karlsruhe, 76344 Eggenstein-Leopoldshafen, Germany (fax: (+49)7247-808-666; E-mail: crysdata@fizkarlsruhe.de) on quoting their ICSD numbers: 431394 and 431395, respectively.

Simultaneously, one $[Cat]_2[Mg(BH_4)_4]$ derivative showing good solubility in DCM (dichloromethane) ([Cat] = $[Ph_4P]$) has been applied for synthesis of the bimetallic borohydrides containing alkali metal cations, M^+ (M = Li–Cs), and magnesium-bearing anions, $[Mg(BH_4)_{2+x}]^{x-}$. We have utilized the recently reported method of solvent-mediated synthesis of mixed-metal borohydrides,[12,31–33] while anticipating that it might proceed according to the following reaction equation:

$$[Cat]_2[Mg(BH_4)_4] + 2\ M[An] \rightarrow M_2[Mg(BH_4)_4]\downarrow + 2[Cat][An] \quad (1)$$

where [An] = $[Al(OC(CF_3)_3)_4]$ or $[B[3,5\text{-}(CF_3)_2C_6H_3]_4]$ (denoted below as $[Al(pftb)_4]$ and $[BAr^F]$, respectively). For M = Rb, Cs, the mixture of amorphous MBH_4 and novel $M_3[Mg(BH_4)_5]$ derivatives have been obtained and characterized, while for M = Li–K the respective single-metal borohydrides were detected among the products.

Methods

Synthetic procedures

All experiments were performed in an argon atmosphere, using the MBRAUN Labmaster DP glovebox (O_2, H_2O <1 ppm) or the Schlenk-type glassware. The reagents used were fine quality chemicals from Sigma-Aldrich and Katchem. M[Al(pftb)$_4$], M = Li–Cs, salts were prepared as mentioned in ref. 32, while $Mg(BH_4)_2$·1.5DME, $[Ph_4P]_2[Mg(BH_4)_4]$ and $Mg(BH_4)_2$·3THF were synthesized using procedures similar to the reports published before (*cf.* ESI†).[25–27] The metathetic solvent-mediated reactions resulting in mixed-metal borohydrides have been described earlier.[12,31,32] The specific methods of synthesis of mixed-cation borohydrides used in this paper have been summarized in Table 1, while the corresponding detailed synthesis procedures are outlined in the ESI.†

Mechanochemical reactions were carried out in stainless steel vessels using an LMW-S vibrational mill from Testchem (1400 rpm, *ca.* 23.3 Hz). The reactions were usually performed for 30 min in 5 min cycles with LN2 cooling between cycles.

Fourier Transform Infrared (FTIR) spectra were recorded on a Vertex 80v spectrometer (Bruker) in the 4000–400 cm^{-1} range. Anhydrous KBr (200 mg) was used as a pellet material.

Thermal decomposition of the selected samples was investigated using a Netzsch STA 409 PG thermogravimeter (TGA) combined with a differential scanning calorimeter (DSC). Evolved gases were analysed using a Pfeiffer vacuum quadrupole mass spectrometer (MS), QMS 403 C, connected to the TGA/DSC furnace *via* a quartz capillary preheated to 200 °C to avoid condensation of the low-boiling volatiles. The samples were placed inside Al_2O_3 crucibles and measured at a constant 5 °C min^{-1} heating rate, and a spontaneous cooling after the maximum temperature has been reached. High-purity 6N argon has been used as a carrier gas with a constant flow of 80 ml min^{-1}. For obtaining larger amounts of the solid residues, a Carbolite GHA 12/300 furnace with the Ar gas flow, was applied.

X-ray photoelectron spectra (XPS) were recorded on a custom-designed system made by SPECS using monochromatized Al K_α radiation (1486.5 eV). The electron flood gun was used for charge compensation. The samples were loaded to the spectrometer *via* the Ar-filled glovebox (MBraun), with O_2 and H_2O levels <0.5 ppm. The experimental setup has been described earlier.[34] For the XPS results *cf.* ESI.†

Powder X-ray Diffraction (PXD) patterns were collected from the samples sealed inside the 0.3–1 mm capillaries. Two diffractometers were used: PANalytical X'Pert Pro with CoK_α radiation and a Bruker D8 Discover with CuK_α radiation. The following software was used for data analysis: Crystal Sleuth[35] – for displaying PXD patterns and preliminary data analysis; X-Cell[36] (included in Materials Studio from Biovia) – for indexing of reflections; FOX[37] – for structure solution; Vesta[38] and Mercury[39] – for visualization of structures, and simulation of

Table 1 The preparation of $M_x[Mg(BH_4)_{2+x}]$ samples described in this work

M	Reagents [mol. ratio]	Conditions	Crystalline products
Me_4N	$MgCl_2$ + 2$LiBH_4$ + 2$[Me_4N]BH_4$	6 × 5 min milling	$[Me_4N]_2[Mg(BH_4)_4]$, LiCl
	$Mg(BH_4)_2$ + 2$[Me_4N]BH_4$	6 × 5 min milling	$[Me_4N]_2[Mg(BH_4)_4]$, $[Me_4N]BH_4$
	$Mg(BH_4)_2$ + $[Me_4N]BH_4$	6 × 5 min milling	$[Me_4N]_2[Mg(BH_4)_4]$, $[Me_4N]BH_4$ [a]
	$Mg(BH_4)_2$·1.5DME + 2$[Me_4N]BH_4$	16 h stirring in DCM, filtration	$[Me_4N]_2[Mg(BH_4)_4]$, $[Me_4N]BH_4$
nBu_4N	$MgCl_2$ + 2$LiBH_4$ + 2$[n Bu_4N]BH_4$	6 × 5 min milling	$[n Bu_4N]_2[Mg(BH_4)_4]$ [a,b]
	$Mg(BH_4)_2$ + $[n Bu_4N]BH_4$	6 × 5 min milling	$[n Bu_4N]_2[Mg(BH_4)_4]$ [a,b]
	$Mg(BH_4)_2$·1.5DME + 2$[n Bu_4N]BH_4$	24 h stirring in DCM	$[n Bu_4N]_2[Mg(BH_4)_4]$ [b]
Ph_4P	$Mg(BH_4)_2$·1.5DME + 2$[Ph_4P]BH_4$	24 h stirring in DCM, Et_2O extraction	$[Ph_4P]_2[Mg(BH_4)_4]$ [a]
Li	$Mg(BH_4)_2$ + 2$LiBH_4$	8 × 5 min milling	$LiBH_4$ [c]
	1.1$[Ph_4P]_2[Mg(BH_4)_4]$ + 2Li[Al(pftb)$_4$]	30 min stirring in DCM, filtering	$LiBH_4$, LiCl, Li[Al(pftb)$_4$], $[Ph_4P]_2[Mg(BH_4)_4]$ [a]
Na	1.1$[Ph_4P]_2[Mg(BH_4)_4]$ + 2Na$[BAr^F_4]$	30 min stirring in DCM, filtering	Na$[BAr^F_4]$, $NaBH_4$
	1.1$[Ph_4P]_2[Mg(BH_4)_4]$ + 3Na[Al(pftb)$_4$]	30 min stirring in DCM, filtering	Na[Al(pftb)$_4$], $NaBH_4$,
K	$[Ph_4P]_2[Mg(BH_4)_4]$ + 2 K[Al(pftb)$_4$]	1–2 h stirring in DCM, filtering	KBH_4
Rb	$[Ph_4P]_2[Mg(BH_4)_4]$ + 2Rb[Al(pftb)$_4$]	19 h stirring in DCM, filtering	$Rb_3Mg(BH_4)_5$
Cs	$Mg(BH_4)_2$ + 2$CsBH_4$	8 × 5 min milling	[c]
	1.1$[Ph_4P]_2[Mg(BH_4)_4]$ + 2Cs[Al(pftb)$_4$]	22 h stirring in DCM, filtering	$Cs_3Mg(BH_4)_5$
	$MgCl_2$ + 2$LiBH_4$ + 3$CsBH_4$	8 × 5 min milling	$Cs_3Mg(BH_4)_5$, LiCl

[a] Unidentified phase(s) present. [b] The crystal structure not solved. [c] Quasi-amorphous products.

powder patterns; Jana2006 [40] – for Rietveld and LeBail refinement. The shape of diffraction peaks has been described as a pseudo-Voigt function with added Berar–Baldinozzi type asymmetry. The background was modeled by using 30 Legendre polynomials. During the Rietveld refinement of all structures the restraints were applied to BH_4^- groups: the B–H distances and the H–B–H angles were fixed to 1.150(1) Å and 109.47(1)°, respectively. Atomic displacement parameters of B atoms were fixed to be equal, while for H atoms they were fixed as 1.2 times larger than that of the B atoms. Mg–H distances were restrained to be equal to each other within ~0.001 Å.

Single-crystal X-ray diffraction measurement and structure solution of $Mg(BH_4)_2$·1.5DME

The measurement was performed at 100(2) K on a Bruker D8 Venture Photon100 CMOS diffractometer equipped with a mirror monochromator and a CuKα INCOATEC IμS microfocus source. Frames were collected using a Bruker APEX2 program[41] and integrated in the Bruker SAINT software package[42] using a narrow-frame algorithm. The integration of the data (cubic unit cell) yielded a total of 49 819 reflections to a maximum θ angle of 58.95° (0.90 Å resolution), of which 5027 were independent (average redundancy 9.910, completeness = 100.0%, R_{int} = 5.10%, R_{sig} = 2.48%) and 4220 (83.95%) were greater than $2\sigma(F^2)$. The final cell parameters of a = 27.2332(9) Å and V = 20 197(2) Å^3 are based on the refinement of the XYZ-centroids of 9916 reflections above 20 $\sigma(I)$ with 5.621° < 2θ < 116.948°. Data were corrected for absorption effects using the multi-scan method (SADABS).[43] The ratio of minimum to maximum apparent transmission was 0.829. The calculated minimum and maximum transmission coefficients (based on crystal size) are 0.768 and 0.856, respectively.

The structure was solved and refined using the SHELXTL software package[44] in the space group $Pa\bar{3}$, with Z = 4 for the formula unit, $C_{96}H_{353}B_{32}Mg_{16}O_{48}$. The final anisotropic full-matrix least-squares refinement on F^2 with 542 variables converged at R_1 = 6.52%, for the observed data and wR_2 = 21.62% for all data. The goodness-of-fit was 1.038. The largest peak in the final difference electron density synthesis was 0.291 e$^-$ Å^{-3} and the largest hole was −0.362 e$^-$ Å^{-3} with an RMS deviation of 0.073 e$^-$ Å^{-3}. The measured crystal was twinned by merohedry with a twin composition plane being a diagonal of a square of the unit cell *i.e.* (110). The refined ratio of twin components is equal to 0.840(2) : 0.160(2). Due to the severe disorder the crystal was weakly diffracting, the resolution of the data was limited to 0.9 Å (maximum 2θ up to 116.9°). A number of constraints for distances and angles were used to model correct geometry of BH_4^- and DME ligands. In both $Mg[(BH_4)_4]^{2-}$ anions and the $Mg[(C_4H_{10}O_2)_3]^{2+}$ cation located on the general position all non-hydrogen atoms were refined anisotropically. In the other cations only Mg and O atoms were refined anisotropically whereas C atoms were refined with an isotropic approach. Hydrogen atoms were placed in calculated positions and refined within the riding model. In one $Mg[(C_4H_{10}O_2)_3]^{2+}$ cation (Mg4 as central ion) hydrogen atoms were not assigned what causes the discrepancy between the atom count from the atom list and the given formula of the investigated salt. The temperature factors of the assigned hydrogen atoms were not refined and were set to be equal to either 1.2 or 1.5 times larger than U_{eq} of the corresponding heavy atom. The atomic scattering factors were taken from the International Tables.[45]

Results and discussion

Synthesis and identification of the products

Organic derivatives of $Mg(BH_4)_2$. The syntheses of $Mg(BH_4)_2$·1.5DME and $Mg(BH_4)_2$·3THF solvates, as well as that of $[Ph_4P]_2[Mg(BH_4)_4]$, result in rather pure products with only small amounts of unidentified impurities (Fig. S1 and S2†). We have also prepared $[Me_4N]_2[Mg(BH_4)_4]$ *via* four different synthetic paths, however, due to its poor solubility in organic solvents, this compound could not be purified (*cf.* Table 1 and Fig. S3†). The synthesis of $[n\mathrm{Bu}_4\mathrm{N}]_2[Mg(BH_4)_4]$ has been attempted using three different methods (Table 1). The products are characterized by the common set of diffraction reflections, accompanied by unidentified peaks for the mechanochemically-synthesized samples (Fig. S4†). The common set of diffraction peaks can be indexed in a tetragonal body-centered unit cell (extinction class $I4_1/a$), a = 25.459(10) Å and c = 34.407(14) Å, V = 22 302(18) Å^3, which is very close to the volume estimated for 20 $[n\mathrm{Bu}_4\mathrm{N}]_2[Mg(BH_4)_4]$ molecules. Moreover, a very similar unit cell is obtained from indexing of the powder pattern for the related manganese derivative, $[n\mathrm{Bu}_4\mathrm{N}]_2[Mn(BH_4)_4]$ (Fig. S29†). Although such a unit cell corresponds very well to the measured powder pattern (Fig. S5†), we failed to solve the crystal structure of this compound from powder diffraction data.[46] Unfortunately, and despite many attempts, we were also unable to grow the crystals suitable for single-crystal diffraction, therefore $[n\mathrm{Bu}_4\mathrm{N}]_2[Mg(BH_4)_4]$ remains to be structurally characterized in the future.

Since $[Ph_4P]_2[Mg(BH_4)_4]$ may be obtained as a quite pure crystalline product, and it shows very good solubility in DCM, we have chosen this compound as a precursor for synthesis of inorganic mixed-cation borohydrides of magnesium.

Inorganic bimetallic borohydrides of magnesium. We attempted preparation of novel mixed-metal borohydrides of magnesium according to eqn (1). The precipitates formed *via* metathetic reactions in DCM were analyzed with powder X-ray diffraction (PXD) and Fourier-transform infrared spectroscopy (FTIR), *cf.* Fig. 1 and 2, respectively.

Surprisingly, we have not detected the $M_2[Mg(BH_4)_4]$ salts in any of the investigated systems, *cf.* Table 1. In the samples containing lighter alkaline metals, M = Li–K, the products were composed of crystalline MBH_4 and amorphous $Mg(BH_4)_2$, as suggested by the PXD patterns and FTIR spectra. In these samples the unreacted M[An] precursors were also present, particularly for M = Na (see also Fig. S6–S13†). These results suggest that the $M_2[Mg(BH_4)_4]$ phases, M = Li–K are either unstable, or they decompose during synthesis:

$$M_2[Mg(BH_4)_4] \rightarrow Mg(BH_4)_2 + 2MBH_4. \quad (2)$$

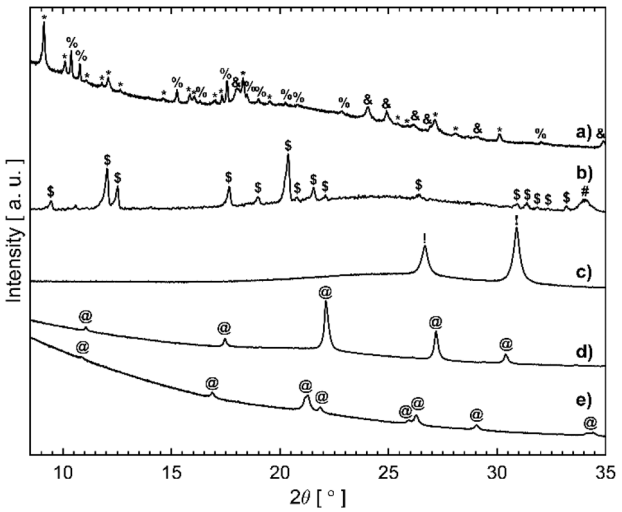

Fig. 1 PXD (Cu Kα) of the $M_x[Mg(BH_4)_{2+x+}]$ compounds for M = (a) Li, freshly-prepared sample; (b) Na; (c) K; (d) Rb; (e) Cs. * – Unknown phase; % – Li[Al(pftb)$_4$]; & – $LiBH_4$; $ – Na[Al(pftb)$_4$]; # – $NaBH_4$; ! – KBH_4; @ – $M_3Mg(BH_4)_5$, M = Rb, Cs.

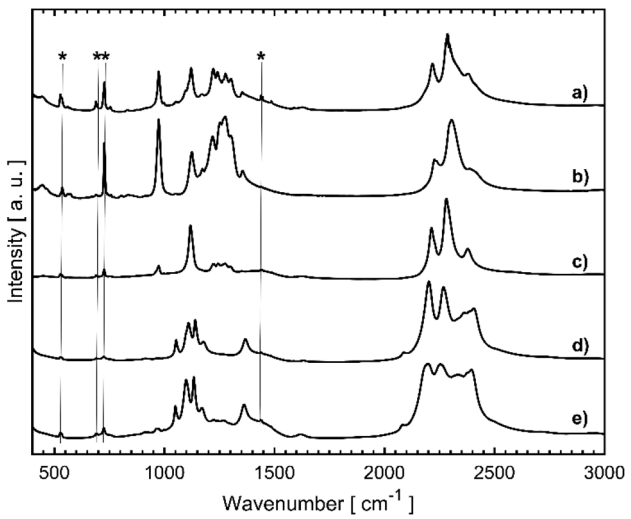

Fig. 2 FTIR spectra of the $M_x[Mg(BH_4)_{2+x+}]$ compounds for *A* = (a) Li, freshly-prepared sample; (b) Na; (c) K; (d) Rb; (e) Cs. * bands from $[Ph_4P]_2Mg(BH_4)_4$.

The lack of thermodynamic stability of $Li_2[Mg(BH_4)_4]$ and $Na_2[Mg(BH_4)_4]$, with respect to the corresponding single-cation borohydrides, might be expected, as no lithium- and sodium-containing bimetallic magnesium borohydrides have been reported.[47–49] This could be rationalized especially for the compound of lithium which, similarly to Mg, shows clear preference for tetrahedral coordination, influencing the topology of a system.[50] Such a strong preference in coordination mode induces incompatibility with the chemical composition required for the charge balance, as it has been discussed by Schouwink *et al.*[23] This incompatibility could be overcome by partial substitution of lithium by potassium or rubidium, acting as counter-cations *e.g.* in $ALiMg(BH_4)_4$, A = K, Rb. Surprisingly, the solvent-mediated synthesis of magnesium-potassium borohydrides appeared unsuccessful, despite the preparation of the stable $K_2[Mg(BH_4)_4]$ and $K_3[Mg(BH_4)_5]$ phases by a mechanochemical process.[22]

In the case of the heavier alkali metals, M = Rb and Cs, the corresponding $M_3Mg(BH_4)_5$ salts are precipitated (Fig. 1d and e). Fig. 2d and e, being the only crystalline phases present in the samples. A band of moderate intensity is observed in their FTIR spectra at *ca.* 1266 cm^{-1}, likely originating from the δ_{H-B-H} absorption band of amorphous $Mg(BH_4)_2$.[51] These observations indicate that the targeted $M_2[Mg(BH_4)_4]$ salts, M = Rb, Cs, either do not form, or they decompose *in situ* according to the eqn (3):

$$3M_2[Mg(BH_4)_4] \rightarrow 2M_3Mg(BH_4)_5 + Mg(BH_4)_2. \quad (3)$$

In this case the MBH_4 are not eliminated, contrary to the compounds of lighter metals, eqn (2), which should be related to significantly lower lattice energies of the heavier alkaline borohydrides.[52]

For comparison, the $Cs_3Mg(BH_4)_5$ salt has also been prepared *via* a mechanochemical reaction:

$$MgCl_2 + 2LiBH_4 + 3CsBH_4 \rightarrow Cs_3Mg(BH_4)_5 + 2LiCl, \quad (4)$$

which resulted in a LiCl-contaminated product of poor crystallinity (Fig. S14†). A mechanochemical attempt towards the preparation of $Cs_2[Mg(BH_4)_4]$:

$$Mg(BH_4)_2 + 2CsBH_4 \rightarrow Cs_2[Mg(BH_4)_4], \quad (5)$$

led to ill-defined, nearly-amorphous products (Fig. S14 and S15†). The recently reported $Cs[Mg(BH_4)_3]$ phase[21] has not been detected in any of our cesium-containing samples.

Crystal structures

$Mg(BH_4)_2$·1.5DME. As discussed above, $Mg(BH_4)_2$ solvated by DME is a useful intermediate for preparation of $[Cat]_2[Mg(BH_4)_4]$ compounds, [Cat] = [Me_4N], [nBu_4N], [Ph_4P], *etc.* Although the synthesis of this compound has been reported before,[26] its structure remained unknown.

$Mg(BH_4)_2$·1.5DME adopts a large primitive cubic unit cell, $Pa\bar{3}$, with a = 27.2332(9) and V = 20 197(2) Å^3 at 100 K, Table S2† (a = 27.5917(6) and V = 21 005.6(5) Å^3, at room temperature, RT, Fig. S16†). The structure is severely disordered and its asymmetric part contains one $Mg[(C_4H_{10}O_2)_3]^{2+}$ cation occupying the general position (24d) and two such cations located at the inversion center of the −3-fold axis of symmetry (4a, 4b). These cations are counterbalanced by one Mg $[(BH_4)_4]^{2-}$ anion located on the general position (24d) and the same type of anion positioned on the −3-fold axis but not on the center of inversion (8c) (Fig. 3). Rather weak interactions between ions together with the disorder are responsible for a relatively small density of the crystal of 0.99 g cm^{-3} at 100 K (0.95 g cm^{-3} at RT).

In the $Mg[(BH_4)_4]^{2-}$ moiety located on the general position one of the BH_4 ligands is disordered over two positions with

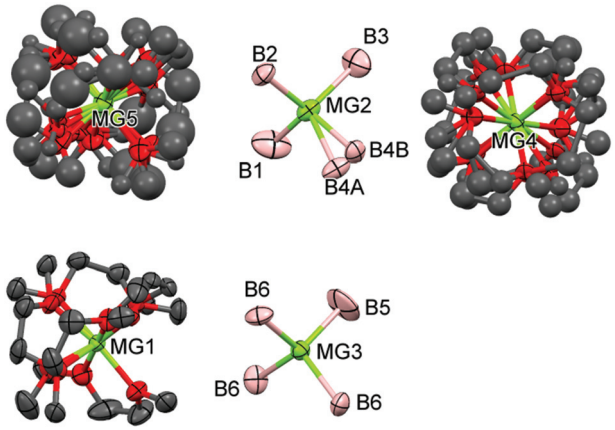

Fig. 3 The asymmetric part of the unit cell of $Mg(BH_4)_2$·1.5DME. The displacement ellipsoids are shown at 50% probability level; Mg – green, B – pink, O – red, and C – grey.

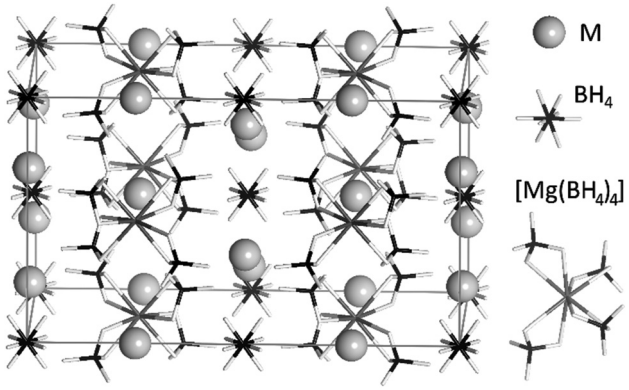

Fig. 4 Unit cell of $M_3Mg(BH_4)_5$, M = Rb, Cs.

the occupancy ratio of 0.5 : 0.5. The second $Mg[(BH_4)_4]^{2-}$ ion is ordered.

The cation moieties contain disordered DME ligands which chelate the central metal ion. In the Mg1 cation one DME molecule is ordered whereas the two other molecules are disordered over two sites with an occupancy ratio equal to 0.55 : 0.45. The other two cations located on the – 3-fold axes contain DME ligands distributed over many alternative positions imposed by the high symmetry of the site occupied by the Mg central ions.

The coordination of magnesium cations is typical of its complexes with BH_4^- and ether ligands, with the Mg–B and Mg–O distances within the range of 2.29(10)–2.447(10) Å and 1.92(2)–2.206(9) Å, respectively.

$M_3Mg(BH_4)_5$, M = Rb, Cs. The diffraction peaks originating from $M_3Mg(BH_4)_5$, M = Rb, Cs has been indexed in tetragonal unit cells with an extinction class of *I4cm* (Table S3†). $K_3Mg(BH_5)_5$ crystallizes in a similar unit cell, however, in this case a loss of body centering is indicated by a set of weak Bragg signals observed below 367 K.[22] We have not detected such signals above the noise level, therefore we refined $M_3Mg(BH_4)_5$, M = Rb, Cs, in the Cs_3CoCl_5-type structure (space group *I4/mcm*),[53] adopted also by using $K_3Mg(BH_5)_5$ at an elevated temperature (Fig. 4, *cf.* Fig. S19 and S20†). This structure has been described as an intergrowth of MBH_4 and $M_2[Mg(BH_4)_4]$; it contains the $[Mg(BH_4)_4]^{2-}$ anions (where Mg^{2+} is coordinated tetrahedrally by four bidentate BH_4^- groups) and the disordered BH_4^- anions (coordinated octahedrally by M^+ cations, like in some MBH_4 phases).[22]

The geometry of the $[Mg(BH_4)_4]^{2-}$ anions for both Rb- and Cs-containing compounds closely resembles that found in the K analogue: the shortest Mg–B distances range from 2.410(10) Å and 2.434(5) to 2.437(8) Å for M = Cs, Rb, and K, respectively, while the corresponding B–Mg–B angles differ not more than 6° among these compounds.[22] The equatorial M1–B2 distances of 3.4402(18) Å (M = Rb) and 3.6003(14) Å (M = Cs), as in the case of $K_3Mg(BH_5)_5$, are slightly shorter than those found in simple MBH_4 salts: 3.5145(5) Å and 3.7095(5) Å, respectively.[54] The apical M2–B2 distances are significantly larger than the equatorial ones, 3.9983(12) Å and 4.0631(4) Å for M = Rb and Cs, respectively, however, this distance depends strongly on the applied model of disorder. Although initially the models of disorder related to that applied before for $K_3Mg(BH_5)_5$ [22] have been tested, they have converged to the structure with the fully ordered heavy atom sublattice.

Thermal decomposition

Organic derivatives of magnesium borohydride. Since $Mg(BH_4)_2$ is a valuable precursor towards superconducting MgB_2, we have studied here the thermal decomposition of the organic derivatives of magnesium borohydride. Of particular interest are $Mg(BH_4)_2$·1.5DME, $Mg(BH_4)_2$·3THF, and $[Ph_4P]_2[Mg(BH_4)_4$, which are very well soluble in a broad range of organic solvents, and as such they might constitute useful precursors towards thin layers of MgB_2 on neutral substrates of any shape.

Thermal decomposition of the organic derivatives of magnesium borohydride is a complex, multistep process, as commonly observed for metal borohydrides (Fig. 5). Heating of the solvates results in partial elimination of the solvent in the first complex endothermic step close to 135 and 70 °C for $Mg(BH_4)_2$·1.5DME and $Mg(BH_4)_2$·3THF, respectively. The mass released from $Mg(BH_4)_2$·1.5DME in the first step of thermal decomposition, *ca.* 23.8 wt%, corresponds to 0.5 formula weight of DME per one formula unit, which confirms the previous observation of the formation of $Mg(BH_4)_2$· DME on heating above 140 °C.[25] In the case of $Mg(BH_4)_2$·3THF the first group of DSC signals, 45–150 °C, corresponds to 26.7 wt% of the mass drop on the TGA curve, which is an equivalent of one molecule of THF per formula unit; thus $Mg(BH_4)_2$·2THF is formed. Further heating of both solvates results in a gradual loss of the solvent without significant heat effects, while close to 250 °C the exothermic processes are observed during which elimination of the solvent fragments together with hydrogen is detected using temperature-resolved MS, Fig. S23 and S24.† During further heating up to *ca.* 450 °C the mass drops further, which, especially for $Mg(BH_4)_2$·1.5DME, is related to

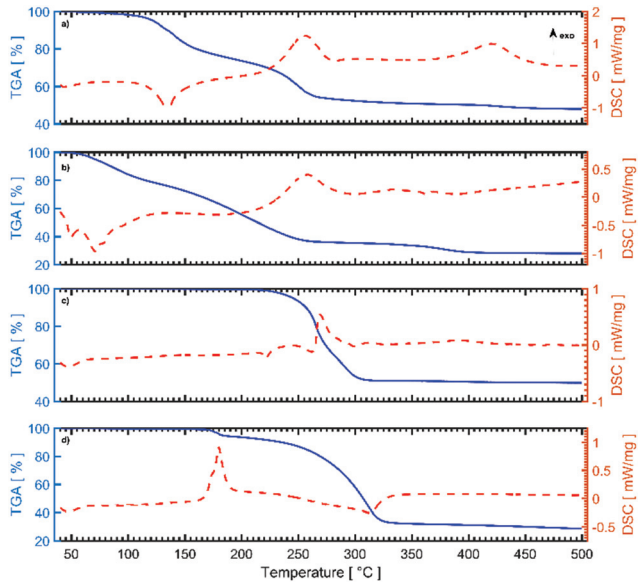

Fig. 5 TGA/DSC profiles: (a) $Mg(BH_4)_2$·1.5DME, (b) $Mg(BH_4)_2$·3THF, (c) $[Me_4N]_2[Mg(BH_4)_4]$ containing 27 wt% LiCl, (d) $[Ph_4P]_2[Mg(BH_4)_4]$. A heating rate of 5 °C min^{-1} was applied.

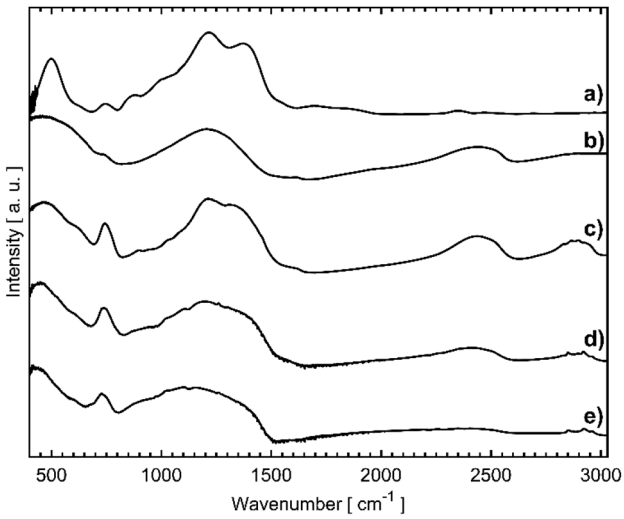

Fig. 6 FTIR spectra of: (a) commercially available MgB_2 (Sigma-Aldrich), (b) $Mg(BH_4)_2$·3THF heated to 500 °C, (c) $Mg(BH_4)_2$·1.5DME heated to 450 °C, (d) $Mg(BH_4)_2$·1.5DME heated to 500 °C, (e) $Mg(BH_4)_2$·1.5DME heated to 650 °C.

the exothermic processes. The total mass losses upon heating to 500 °C, *i.e.* 52.1 wt% and 71.9 wt%, for $Mg(BH_4)_2$·1.5DME and $Mg(BH_4)_2$·3THF, respectively, are too small if pure MgB_2 is expected.

The organic mixed-cation borohydrides containing magnesium start to decompose at significantly higher temperatures than the solvates (Fig. 5c and d). In the case of $[Me_4N]_2[Mg(BH_4)_4]$ several endo- and exothermic DSC events contribute to the major mass loss as observed over the temperature range 200–300 °C. The processes taking place during thermal decomposition of $[Ph_4P]_2[Mg(BH_4)_4]$ are better separated and include the exothermic events close to 180 °C, related to the minor mass loss, and endothermic processes, with simultaneous gradual mass loss over 225–330 °C. During thermal decomposition of these two compounds, both hydrogen and various organic fragments are detected using temperature-resolved MS, Fig. S21 and S22.† The masses of the solid residue after heating of the samples of $[Me_4N]_2[Mg(BH_4)_4]$ (containing 27 wt% LiCl) and $[Ph_4P]_2[Mg(BH_4)_4]$ up to 500 °C are equal to 50 wt% and 28.9 wt% respectively, and they are significantly larger than those expected for thermal decomposition yielding pure MgB_2 of 35.5 wt% (including the mass of LiCl) and 10.9 wt%, respectively.

The solid residues of the thermal decomposition of $Mg(BH_4)_2$·1.5DME and $Mg(BH_4)_2$·3THF solvates were further characterized with PXD and FTIR. For both samples no Bragg peaks (besides the signals of contamination), but rather the broad humps signaling amorphous materials are observed (Fig. S25 and S28†). Simultaneously, the main FTIR absorption bands of the residues below 1500 cm^{-1} resemble those of MgB_2,[55,56] which is especially well visible for the samples heated to 450 and 500 °C (Fig. 6). At higher wavenumbers the absorption bands from the MgB_2 impurities are observed: the band around 2400 cm^{-1} is characteristic for the ν_{B-H} vibrations of partly decomposed B_xH_y compounds, while those around 2900 cm^{-1} correspond to the ν_{C-H} stretches from the organic species present in the residues. The intensity of the signals coming from impurities diminishes with the increasing maximum temperature of the thermal decomposition, but they are present even for the samples heated up to 650 °C – a temperature above which thermal decomposition of MgB_2 accelerates[57] (*cf.* Fig. 6e).

The formation of MgB_2 during thermal decomposition of $Mg(BH_4)_2$·1.5DME heated to 450 °C has been further confirmed *via* magnetometric measurements, which clearly showed signatures of a superconducting phase with the critical superconducting temperature around 39 K, as well as the presence of some unidentified paramagnetic impurities.[58] These results taken together show that solvates of $Mg(BH_4)_2$ may in principle be used for obtaining MgB_2, but the product is amorphous and contains substantial amounts of organic and inorganic impurities.

Inorganic derivatives: $M_3Mg(BH_4)_5$, M = Rb, Cs. Thermal decomposition of $M_3Mg(BH_4)_5$, M = Rb, Cs, has also been studied. Since – as described above – the samples inevitably contain substantial amounts of amorphous $Mg(BH_4)_2$, it is difficult to unequivocally associate various observed thermal and mass loss signatures with the phases of interest. Hence, the discussion of the thermal decomposition of these samples has been presented in the ESI.†

Conclusions

In this work we have reported synthesis and physicochemical characterization of the five organic derivatives of magnesium

borohydride, namely two solvates: $Mg(BH_4)_2$·1.5DME and $Mg(BH_4)_2$·3THF and three mixed-cation borohydrides, $[Cat]_2[Mg(BH_4)_4]$, [Cat] = [Me_4N], [nBu_4N], and [Ph_4P]. The latter compound has served as a precursor in the synthetic attempts towards the series of mixed-metal borohydrides of magnesium, $M_2[Mg(BH_4)_4]$, M = Li–Cs according to the recently reported solvent-mediated method.[12] This synthetic approach has failed for M = Li, Na and K since only the corresponding MBH_4 (M = Na, K) together with unidentified products (M = Li) and unreacted precursors have been detected. The reactions took a different course for the heavier alkali metals (M = Rb, Cs) yielding a mixture of crystalline $M_3Mg(BH_4)_5$ and amorphous $Mg(BH_4)_2$. Contrastingly to the numerous mixed-metal borohydrides, which could be conveniently prepared using this path of synthesis,[32] the targeted $M_2[Mg(BH_4)_4]$ borohydrides could not be achieved using a metathetic approach.

Most of the organic borohydrides described here reveal excellent solubility in diverse organic solvents therefore we have initially evaluated if these compounds might be convenient precursors towards thin layers of an MgB_2 superconductor. According to our thermogravimetric measurements the solid products of thermal decomposition of organic derivatives of magnesium borohydride contain amorphous MgB_2, which is contaminated with organic and inorganic species. Therefore further investigation is needed to obtain MgB_2 of high purity using those or modified precursors.[28]

Acknowledgements

This research was financed from the NCN project UMO-2014/15/B/ST5/05012. Research was carried out with the use of CePT infrastructure financed by the European Union – the European Regional Development Fund within the Operational Programme "Innovative economy" for 2007–2013 (POIG.02.02.00-14-024/08-00). The X-ray measurement was performed in the Czochralski Laboratory of Advanced Crystal Engineering (Department of Chemistry, University of Warsaw) established by generous support from the Polish Ministry of Science and Higher Education (grant No. 614/FNiTP/115/2011). The authors wish to thank Michał Tyszkiewicz for sharing the PXRD pattern of $[nBu_4N]_2[Mn(BH_4)_4]$.

This paper commemorates the 200th anniversary of The University of Warsaw.

Notes and references

1 M. S. Dresselhaus and I. L. Thomas, *Nature*, 2001, **414**, 332.
2 W. Grochala and P. P. Edwards, *Chem. Rev.*, 2004, **104**, 1283.
3 U. Eberle, M. Felderhoff and F. Schüth, *Angew. Chem., Int. Ed.*, 2009, **48**, 6608.
4 A. J. Churchard, E. Banach, A. Borgschulte, R. Caputo, J.-C. Chen, D. Clary, K. J. Fijalkowski, H. Geerlings, R. V. Genova, W. Grochala, T. Jaroń, J. C. Juanes-Marcos, B. Kasemo, G. J. Kroes, I. Ljubic, N. Naujoks, J. K. Nørskov, R. A. Olsen, F. Pendolino, A. Remhof, L. Romanszki, A. Tekin, T. Vegge, M. Zach and A. Züttel, *Phys. Chem. Chem. Phys.*, 2011, **13**, 16955.
5 Q. Lai, A. W. Thornton, M. R. Hill, Z. Haung, H. K. Lui, Z. Guo, M. Paskevicius, D. A. Sheppard, C. Buckley, A. Banerjee, S. Chakraborty, R. Ahuja and K. F. Aguey-Zinsou, *ChemSusChem*, 2015, **8**, 2789.
6 One of the triggers was the discovery of catalytically-enhanced reversible hydrogen storage in alanates: B. Bogdanović and M. Schwickardi, *J. Alloys Compd.*, 1997, **253–254**, 1.
7 T. Jaroń, W. Wegner and W. Grochala, *Dalton Trans.*, 2013, **42**, 6886.
8 M. Chong, E. Callini, A. Borgschulte, A. Züttel and C. M. Jensen, *RSC Adv.*, 2014, **4**, 63933.
9 R. Černý and P. Schouwink, *Acta Crystallogr., Sect. B: Struct. Sci.*, 2015, **71**, 619.
10 H. Hagemann and R. Černý, *Dalton Trans.*, 2010, **39**, 6006.
11 M. B. Ley, M. Paskevicius, P. Schouwink, B. Richter, D. A. Sheppard, C. E. Buckley and T. R. Jensen, *Dalton Trans.*, 2014, **43**, 13333.
12 T. Jaroń, P. Orłowski, W. Wegner, K. J. Fijałkowski, P. J. Leszczyński and W. Grochala, *Angew. Chem., Int. Ed.*, 2015, **54**, 1236.
13 According to the Web of Science there are 145 papers related to "magnesium borohydride" published in the last five years (status for 16 May 2016).
14 K. Chłopek, C. Frommen, A. Léon, O. Zabara and M. Fichtner, *J. Mater. Chem.*, 2007, **17**, 3496.
15 P. Zanella, L. Crociani, N. Masciocchi and G. Giunchi, *Inorg. Chem.*, 2007, **46**, 9039.
16 Y. Filinchuk, R. Černý and H. Hagemann, *Chem. Mater.*, 2009, **21**, 925.
17 J.-H. Her, P. W. Stephens, Y. Gao, G. L. Soloveichik, J. Rijssenbeek, M. Andrus and J.-C. Zhao, *Acta Crystallogr., Sect. B: Struct. Sci.*, 2007, **63**, 561.
18 Y. Filinchuk, B. Richter, T. R. Jensen, V. Dmitriev, D. Chernyshov and H. Hagemann, *Angew. Chem., Int. Ed.*, 2011, **50**, 11162.
19 O. Zavorotynska, A. El-Kharbachi, S. Deledda and B. C. Hauback, *Int. J. Hydrogen Energy*, 2016, **41**, 14387.
20 R. Černý, N. Penin, V. D'Anna, H. Hagemann, E. Durand and J. Růžička, *Acta Mater.*, 2011, **59**, 5171.
21 P. Schouwink, M. B. Ley, A. Tissot, H. Hagemann, T. R. Jensen, L. Smrčok and R. Cěrný, *Nat. Commun.*, 2014, **5**, 5706.
22 P. Schouwink, V. D'Anna, M. B. Ley, L. M. Lawson Daku, B. Richter, T. R. Jensen, H. Hagemann and R. Černý, *J. Phys. Chem. C*, 2012, **116**, 10829.
23 P. Schouwink, M. B. Ley, T. R. Jensen, L. Smrčok and R. Černý, *Dalton Trans.*, 2014, **43**, 7726.
24 R. Černý, P. Schouwink, Y. Sadikin, K. Stare, L. Smrčok, B. Richter and T. R. Jensen, *Inorg. Chem.*, 2013, **52**, 9941.
25 V. D. Makhaev, A. P. Borisov, A. S. Antsyshkina and G. G. Sadikov, *Russ. J. Inorg. Chem.*, 2004, **49**, 323, (*Zh. Neorga. Khim.*, 2004, **49**, 371). Translated from.

26 E. B. Lobkovskii, L. V. Titov, S. B. Psikha, M. Yu. Antipin and Yu. T. Struchkov, *Zh. Strukt. Khim.*, 1982, **23**, 174.
27 H. Nöth, *Z. Naturforsch., B: Anorg. Chem. Org. Chem.*, 1982, **87**, 1499.
28 J. Yang, J. Zheng, X. Zhang, Y. Li, R. Yang, Q. Feng and X. Li, *Chem. Commun.*, 2010, **46**, 7530.
29 H. Fuji and K. Ozawa, *Supercond. Sci. Technol.*, 2010, **23**, 125012.
30 L. P. Chen, C. Zhang, Y. B. Wang, Y. Wang, Q. R. Feng, Z. Z. Gan, J. Z. Yang and X. G. Li, *Supercond. Sci. Technol.*, 2011, **24**, 015002.
31 T. Jaroń, W. Wegner, K. J. Fijałkowski, P. J. Leszczyński and W. Grochala, *Chem. – Eur. J.*, 2015, **21**, 5689.
32 A. Starobrat, M. J. Tyszkiewicz, W. Wegner, D. Pancerz, P. A. Orłowski, P. J. Leszczyński, K. J. Fijalkowski, T. Jaroń and W. Grochala, *Dalton Trans.*, 2015, **44**, 19469.
33 T. Jaroń, W. Wegner and W. Grochala, *Polish patent application*, P.405397, 2013; T. Jaroń, W. Wegner and W. Grochala, *PCT patent application*, PCT/IB2014/001884, 2014.
34 A. Grzelak, T. Jaroń, Z. Mazej, T. Michałowski, P. Szarek and W. Grochala, *J. Electron Spectrosc. Relat. Phenom.*, 2015, **202**, 38.
35 T. Laetsch and R. T. Downs, Software For Identification and Refinement of Cell Parameters From Powder Diffraction Data of Minerals using the RRUFF Project and American Mineralogist Crystal Structure Databases. Abstracts from the 19th General Meeting of the International Mineralogical Association, Kobe, Japan, 23–28 July 2006, 2006.
36 M. Neumann, *J. Appl. Crystallogr.*, 2003, **36**, 356.
37 V. Favre-Nicolin and R. Černý, *J. Appl. Crystallogr.*, 2002, **35**, 734.
38 K. Momma and F. Izumi, *J. Appl. Crystallogr.*, 2011, **44**, 1272.
39 http://www.ccdc.cam.ac.uk/Solutions/CSDSystem/Pages/Mercury.aspx.
40 V. Petricek, M. Dusek and L. Palatinus, *Z. Kristallogr.*, 2014, **229**, 345.
41 *APEX2*, Bruker AXS Inc., Madison, Wisconsin, USA, 2013.
42 *SAINT*, Bruker AXS Inc., Madison, Wisconsin, USA, 2013.
43 *SADABS*, Bruker AXS Inc., Madison, Wisconsin, USA, 2012.
44 G. M. Sheldrick, *Acta Crystallogr., Sect. A: Fundam. Crystallogr.*, 1990, **46**, 467; G. M. Sheldrick, *Acta Crystallogr., Sect. A: Fundam. Crystallogr.*, 2008, **64**, 112.
45 *International Tables for Crystallography*, ed. A. J. C. Wilson, Kluwer, Dordrecht, 1992, vol. C.
46 For the analogous Mn-containing compound the LeBail fit of the experimental PXD data to the mentioned $I4_1/a$ unit cell is even better as the sample contains virtually one crystalline phase. M. Tyszkiewicz, private communication (2016).
47 E. G. Bardají, Z. Zhao-Karger, N. Boucharat, A. Nale, M. J. Van Setten, W. Lohstroh, E. Röhm, M. Catti and M. Fichtner, *J. Phys. Chem. C*, 2011, **115**, 6095.
48 M. B. Ley, E. Roedern, P. M. M. Thygesen and T. R. Jensen, *Energies*, 2015, **8**, 2701.
49 The dual-cation (Li, Mg) borohydride has been claimed in: Z.-Z. Fang, X.-D. Kang, P. Wang, H.-W. Li and S.-I. Orimo, *J. Alloys Compd.*, 2010, **491**, L1. However, formation of the well-defined mixed-cation borohydride in this system has neither been confirmed elsewhere, nor has been confirmed by the reaction performed in our mechanochemical setup, *cf.* ESI.†
50 P. Schouwink, L. Smrčok and R. Černý, *Acta Crystallogr., Sect. B: Struct. Sci.*, 2014, **70**, 871.
51 V. D'Anna, A. Spyratou, M. Sharma and H. Hagemann, *Spectrochim. Acta, Part A*, 2014, **128**, 902.
52 Theoretical investigation of thermodynamics of the reaction (3) could shed some light on the real mechanism, however, it would not be a straightforward task, as the structure of $M_3Mg(BH_4)_5$ is disordered, while the structures of $M_2[Mg(BH_4)_4]$ phases are not known.
53 H. M. Powell and A. F. J. Wells, *J. Chem. Soc.*, 1935, 359.
54 S. C. Abrahams and J. Kalnajs, *J. Chem. Phys.*, 1954, **22**, 434.
55 C. S. Sundar, A. Bharathi, M. Premila, T. N. Sairam, S. Kalavathi, G. L. N. Reddy, V. S. Sastry, Y. Hariharan and T. S. Radhakrishnan, Infrared absorption in superconducting MgB2, 2001, arxiv.org/pdf/cond-mat/0104354.
56 J. A. Alarco, A. Chou, P. C. Talbot and I. D. R. Mackinnon, *Phys. Chem. Chem. Phys.*, 2014, **16**, 24443.
57 Z. Y. Fan, D. G. Hinks, N. Newman and J. M. Rowell, *Appl. Phys. Lett.*, 2001, **79**, 87.
58 A zero field cooling/field cooling (ZFC/FC) magnetometric measurement has been performed for this sample using a SQUID-VSM magnetometer from Quantum Design.

